

**IOCN
2022**

The 3rd International Online-Conference on Nanomaterials

25 APRIL – 10 MAY 2022 | ONLINE

DESIGN OF NANOVESICULAR SYSTEMS FOR MANGIFERIN TRANSDERMAL DELIVERY



nanomaterials



**Maddalena Sguizzato¹, Francesca Ferrara², Paolo Mariani³, Maria Grazia Ortore³, Alessia Pepe³,
Rita Cortesi¹, Mascia Benedusi², Giuseppe Valacchi^{2,4,5*} and Elisabetta Esposito^{1,*}**

¹Department of Chemical and Pharmaceutical Sciences,, University of Ferrara, I-44121 Ferrara, Italy; sgzmdl@unife.it (M.S.); crt@unife.it (R.C.); ese@unife.it (E.E.);

²Department of Neurosciences and Rehabilitation, University of Ferrara, Ferrara; I-44121 Ferrara, Italy; frfrnc3@unife.it (F.F.); bndmsc@unife.it (M.B.); vlcgpp@unife.it (G.V.);

³Department of Life and Environmental Sciences, Università Politecnica delle Marche, I-60131 Ancona, Italy; p.mariani@staff.univpm.it (P.M.); m.g.ortore@staff.univpm.it (M.G.O.); a.pepe@pm.univpm.it (A.P.)

*Correspondence: vlcgpp@unife.it (G.V.); ese@unife.it (E.E.) Tel.: +39-0532-455230



Abstract: Mangiferin is a natural glucosyl xanthone with antioxidant and anti-inflammatory potential that makes it suitable to treat skin diseases. To promote the transdermal administration of mangiferin, phospholipid based vesicular systems, ethosomes and transethosomes, were produced and characterized. The effect of polysorbate 80 and/or poloxamer 407 in transethosome composition was investigated on vesicles size distribution and morphology by photon correlation spectroscopy and transmission electron microscopy. To study the capability of ethosome and transethosome formulations as delivery systems for mangiferin, encapsulation efficiency and in vitro diffusion parameters were evaluated by Franz cells. Mean diameter of vesicles was affected by phosphatidylcholine concentration and by the presence of polysorbate or poloxamer, ranging between 200 and 550 nm. A unilamellar supramolecular structure was detectable in the case of ethosome and polysorbate transethosome, while the presence of poloxamer led to multilamellar structures. The diffusion kinetic of mangiferin was faster in the case of transethosomes produced in the presence of poloxamer. Furthermore, 3D human skin models exposed to ozone enabled to demonstrate the antioxidant and anti-inflammatory effect of mangiferin containing transethosomes against pollutants, especially in the case of vesicles produced in the presence of poloxamer, suggesting their possible application to prevent and treat skin conditions associated to ox-inflammatory mechanisms.

Keywords: ethosomes; transethosomes; mangiferin; Franz cell; antioxidants

Results and Discussion

The nanosystem composition was mainly based on phosphatidylcholine (PC 0.9 or 1.8%) and ethanol 30%, resulting in the production of ethosomes (ETO), while the enrichment of ETO composition with TW₈₀ (0.2 or 0.3%) or P407 (1.2 %) led to transethosomes (TETO) (Table 1). The vesicular dispersions appear homogeneous and milky, translucent in the case of TW₈₀ presence. The loading of mangiferin (MG) MG did not affect the macroscopic aspect of ETO and TETO.

Table 1. Composition of ethosomes and transethosomes.

Formulation	PC ¹ % w/w	Ethanol % w/w	TW ₈₀ ² % w/w	P407 ³ % w/w	MG ⁴ % w/w	Water % w/w
ETO	0.9	29.1	-	-	-	70.0
ETO-MG	0.9	29.1	-	-	0.1	69.9
TETO 1	0.9	28.8	0.3	-	-	69.9
TETO 1-MG	0.89	28.8	0.3	-	0.1	69.9
TETO 2	1.8	17	-	1.2	-	80.0
TETO 2-MG	1.8	16.9	-	1.2	0.1	80.0
TETO 3	1.8	18	0.2	-	-	80.0
TETO 3-MG	1.8	17.9	0.2	-	0.1	80.0

1: phosphatidyl choline; 2: polysorbate 80; 3: poloxamer 407; 4: mangiferin.

Nanosystem size distribution, studied by PCS revealed that mean diameters were related to composition (Table 2). The presence of P407 resulted in vesicles whose mean diameter was almost 50 nm larger with respect to ETO (TETO-2). The addition of MG in ETO and TETO led to a slight reduction of mean diameters. In all cases dispersity indexes were below 0.2, reflecting a narrow size distribution, characterized by almost one vesicle population, as indicated by the typical intensity distribution values.

Table 2. Size distribution parameters of vesicular nanosystems, as determined by PCS.

Formulation	Z-Average (nm) ± s.d. (nm)	Typical Intensity distribution		Dispersity index ± s.d. (nm)
		nm	Area %	
ETO	206.3 ± 33	261 (5065)*	99.5 (0.5)*	0.14 ± 0.04
ETO-MG	189.8 ± 13	178.8 (5049)*	99.6 (0.4)*	0.13 ± 0.02
TETO-1	186.2 ± 20	187.0	100	0.13 ± 0.05
TETO-1-MG	169.3 ± 1	168.7	100	0.13 ± 0.02
TETO-2	253.3 ± 25	255.3	100	0.18 ± 0.04
TETO-2-MG	243.7 ± 22	245.2	100	0.17 ± 0.03
TETO-3	338.5 ± 30	336 (1080)*	99.5 (0.5)*	0.18 ± 0.05
TETO-3-MG	332.5 ± 25	320 (2040)*	99.4 (0.6)*	0.20 ± 0.05

* secondary peak

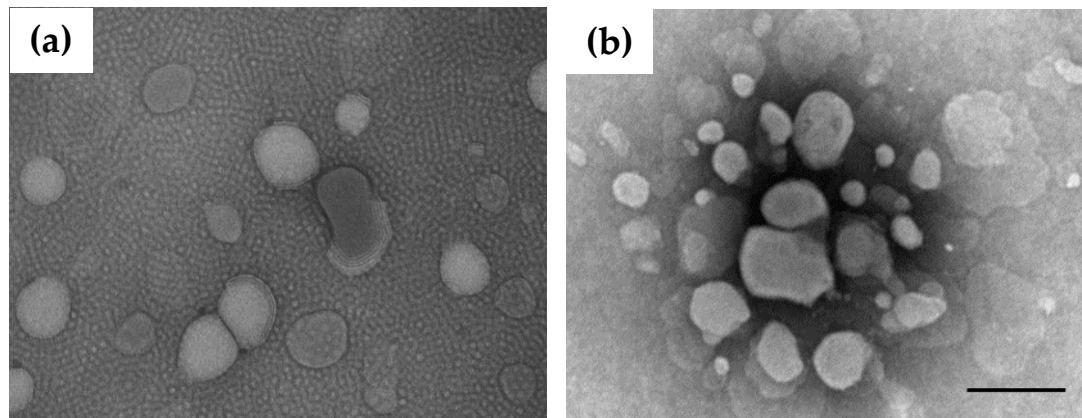


Figure 1. Transmission electron microscopy images (TEM) of TETO-2-MG (a) and TETO-3-MG (b). Bar corresponds to 400 nm.

Table 3. Entrapment capacity and diffusion coefficients of MG loaded in the indicated forms.

Formulation	EC ^a (%)	F ^b (mg/cm ² x h x 10 ³)	D ^c (cm/h x 10 ³)
ETO-MG	78	42.03	42.03
TETO-1-MG	71	67.70	67.70
TETO-2-MG	88	36.82	52.32
TETO-3-MG	87	52.32	36.82
Sol-MG	-	73.02	73.02

^aEntrapment capacity; ^bFlux; ^cDiffusion coefficient; Data are the mean of 6 independent Franz cell experiments

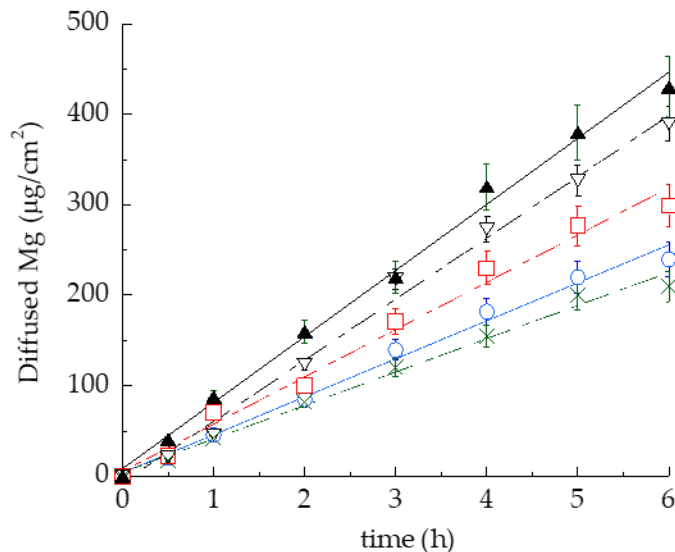


Figure 2. MG diffusion kinetics from Sol-MG (closed triangles), ETO-MG (blue circles), TETO-1-MG (open triangles), TETO-3-MG (red squares), and TETO-2-MG (green crosses), as determined by Franz cell. Experiments were conducted for 6 h. Data are the mean of 6 independent experiments \pm s.d..

Vesicular nanosystems controlled MG diffusion with respect to Sol-MG. D values of vesicular systems followed the order TETO-1-MG > TETO-3-MG > ETO-MG > TETO-2-MG (Table 3). Particularly, on one hand the presence of TW80 (TETO-1-MG) increased MG diffusion with respect to plain ETO-MG, while on the other a double amount of PC associated to P407 enabled to halve D of MG (TETO-2-MG). On the basis of the EE of MG and the capability to restrain MG diffusion, TETO-2-MG and TETO-3-MG were selected for biological studies.

The transdermal potential of TETO-2-MG and TETO-3-MG and their protective effect against pollutants, were studied on 3D human skin models. Particularly, 4HNE protein adducts levels were evaluated in order to gain information on the protective effect of the encapsulated MG, known to counteract the cutaneous O₃-induced oxidative stress damage. 4HNE protein adducts normally occur upon O₃ exposure and represent a marker of lipid peroxidation. After a pretreatment of 3D human skin tissues with TETO-2-MG and TETO-3-MG the tissues were exposed to O₃. The 4HNE protein adducts levels were evaluated by immunofluorescence staining directly post-exposure and 24 h later. The exposure to O₃ induced a significant increase in 4HNE protein adducts levels with respect to untreated tissues exposed to air. The topical administration of TETO-2-MG and TETO-3-MG induced a halving of 4HNE levels, resulting in protection against oxidative stress promoted by O₃ exposure. The effect has been maintained even 24 h after O₃ exposure, suggesting that the vesicles were able to retain MG and prolong its release. Moreover, since the cutaneous oxidative stress is directly related to inflammation on skin upon pollutants exposure, the release of proinflammatory cytokine IL-1 β was measured in 3D skin models to study the inflammatory conditions under O₃ exposure.

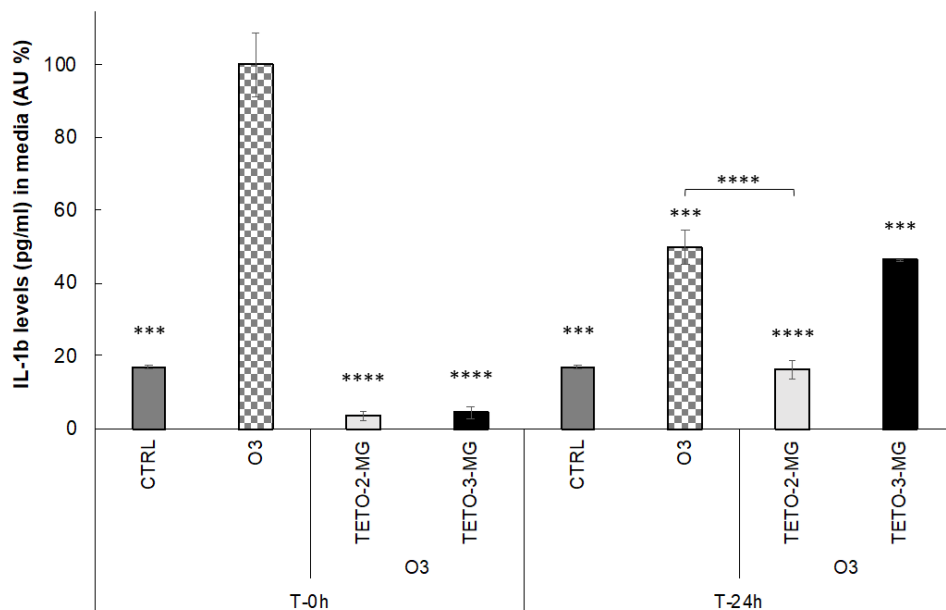


Figure 3. Levels of IL-1 β (pg/mL) in the media of 3D skin models treated with TETO-2-MG and TETO-3-MG analysed using an IL-1 β ELISA kit 0 or 24 h after exposure to O₃ 0.4 ppm for 4 h. Data were normalized with respect to the O₃ sample at 0 h and expressed as arbitrary units (%) \pm SD. Data are the averages of at least three different experiments. *** $p < 0.001$, **** $p < 0.0001$ vs O₃ at T-0 h.

As reported in Figure 3, immediately after exposure to O₃, high levels of IL-1 β were re-released, confirming the inflammatory status of the skin, as compared to CTRL sample.

In the case of TETO-2-MG and TETO-3-MG treatment, low levels of IL-1 β were released, suggesting an almost total protection against O₃ damage. After 24 h, the capability of TETO-2-MG to prevent the O₃ inflammatory damage was even more evident with respect to TETO-3-MG, indicating that TETO-2-MG exerted a longer MG antiinflammatory effect with respect to TETO-3-MG, in agreement with in vitro diffusion data.

Conclusions

This study has demonstrated the suitability of ETO and TETO as delivery systems for MG. Nonetheless, animal models will be required to evaluate the efficacy of TETO-2-MG and TETO-3-MG in the prevention and treatment of cutaneous conditions related to ox-inflammatory mechanisms.

Acknowledgments

We acknowledge Diamond Light Source for time on Beamline I22 under Proposal SM28022. The authors also acknowledge the kind support provided by Olga Shebanova and Tim Snow.

This research was funded by the University of Ferrara, FAR 2020.

